

SECONDARY CYCLOGENESIS ASSOCIATED WITH STRATOSPHERIC INTRUSION OVER THE EAST COAST SOUTH OF BRAZIL

Clara Miho Narukawa Iwabe and Rosmeri Porfírio da Rocha*

Institute of Astronomy, Geophysics and Atmospheric Sciences - University of São Paulo - Brazil

1. Introduction

Several case studies of cyclogenesis in the Northern Hemisphere (NH) have examined the relationship between stratosphere-troposphere interaction and surface cyclone development (Reed and Danielsen, 1959; Danielsen, 1968; Danielsen and Mohnen, 1977; Ancellet et al., 1991; Hoskins et al., 1985). However, in the Southern Hemisphere (SH), this kind of study is still scarce. Miki-Funatsu et al. (2004), investigated a cyclone which developed in the eastern Andes Mountains, indicating that the topography was very important to its initial development as it favored cyclonic vorticity advection and the intensification of a low-level baroclinic zone. For this event, the inversion of PV showed that the low level warm advection was very important to the initial cyclone development.

Holland et al. (1987), after studying three different types of cyclogenesis in the east coast of Australia, registered the type 3 developing near the coast as a secondary cyclone to the rear of a cold front, concluding that this kind of cyclone develops in a region of strong sea surface temperature gradient and considerable low level baroclinicity. The upper tropospheric features indicate that this secondary cyclone initiated and intensified in the vicinity of a tropopause fold.

According to Bosart (1999), Thorncroft et al. (1993) and Davies et al. (1991), PV anomalies were frequently present in the tropopause immediately upstream of the region where the surface cyclone developed. The characteristics of the tropopause are very important for the evolution and intensity of surface cyclones and anticyclones. Therefore, the study of cyclone development from the point of view of upper troposphere, tropopause, and lower stratosphere disturbances is very important to understand the cyclogenesis process in South America.

2. Data Description and Methodology

The NCEP-DOE (National Centers for Environmental Prediction - Department of Energy; Kanamitsu et al., 2002) reanalysis 2 dataset were used. The fields are available every 6 hours (00, 06, 12 and 18 UTC), a horizontal resolution of 2.5 x 2.5 degrees and a vertical resolution of 17 standard pressure levels. TOMS data, provided by British Atmospheric Data Centre (BADC), were used. An analysis of the secondary cyclogenesis initiated at 06 UTC of 17 April 1999 over the eastern coast of South Brazil, in association with an event of stratospheric air

intrusion into the troposphere, is presented in this study. In order to identify this intrusion, the PV was calculated in isobaric vertical coordinates following Reed (1955):

$$PV = -g \left[(\zeta_p + f) \frac{\partial \theta}{\partial p} - \frac{\partial \theta}{\partial x} \frac{\partial v}{\partial p} + \frac{\partial \theta}{\partial y} \frac{\partial u}{\partial p} \right] \quad (1)$$

Where g is the acceleration due to gravity; ζ_p , the vertical component of relative vorticity in isobaric vertical coordinate; f , the Coriolis parameter; θ , the potential temperature, and u and v , the zonal and meridional wind components, respectively. One Potential Vorticity Unit (1 PVU) corresponds to $10^{-6} \text{ m}^2 \text{ s}^{-1} \text{ K kg}^{-1} \text{ PV}$. The presence of a negative PV ($PVU \leq -1.5$) in the upper troposphere of the SH, suggests a negative absolute vorticity anomaly (Bluestein, 1993). In the present study, a threshold of -1.5 PVU was used to characterize the PV anomalies at upper troposphere. In addition to PV, relative humidity, \mathbf{Q} -vector divergence, and ozone measurements were used to characterize the stratospheric air intrusion. The \mathbf{Q} -vector was calculated according to Hoskins (1978) as follows:

$$\mathbf{Q} = (Q_1, Q_2) = \left(-\frac{R}{p} \frac{\partial \bar{V}_g}{\partial x} \cdot \bar{\nabla}_p T, -\frac{R}{p} \frac{\partial \bar{V}_g}{\partial y} \cdot \bar{\nabla}_p T \right) \quad (2)$$

Where, R is the ideal gas constant for dry air, \bar{V}_g , the geostrophic wind, and T , the temperature.

Given the absence of observed vertical profiles of ozone in the area of study, the PV field may be used in order to identify traces of stratospheric ozone (Rondanelli et al., 2002). Larger ozone concentration is supposed to coincide with PV anomalies in the troposphere.

3. Results

3.1 Synoptic Description

The GOES-8 Infra-Red (IR) image at 12 UTC 17 April 1999 (Figure 1) shows two main areas of clouds: the comma-shaped cloud on the eastern coast of South Brazil and the northwest-southeast extended cloud band (centered in 45° S, 30° W). The high pressure center (1028 hPa) to the east of the Andes Mountain has advanced northward, reaching Bolivia, Paraguay, and center-western Brazil. This system favored the incursion of cold air for subtropical South America and, according to Satyamurty et al. (2002), was associated with temperature falls of up to 16° C in 24 hours in some regions, with frosts being registered

*Corresponding author address: Dra Rosmeri Porfírio da Rocha - Rua do Matão - 1226 - Cidade Universitária 05508-090 São Paulo - Brazil
E-Mail: rosmerir@model.iag.usp.br

in the morning of the April 17 in South Brazil. By 06 UTC 17 April it is possible to note the presence of the two low pressure center (Figure 2). The center near of the coast formed at 06 UTC 17 April, which we denominated secondary cyclone and the center to the east developed at 00 UTC 16 April, which we appointed as primary cyclone. At this time, PV anomaly at 300 hPa was nearly in phase with secondary cyclone (Figure 2).

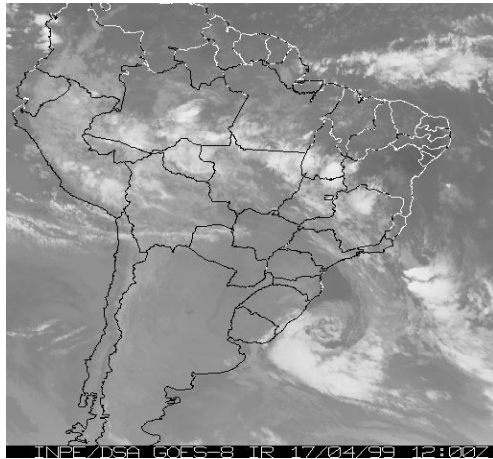


Figure 1. GOES-8 IR image at 12 UTC 17 April 1999.

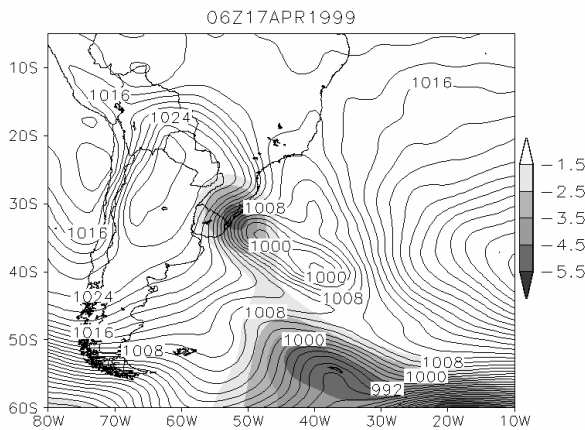


Figure 2. PV anomaly at 300 hPa (PVU, gray shaded showing only negative values) and sea level pressure in 2 hPa intervals (solid line) at 06 UTC 17 April 1999.

Figure 3 presents the trajectory of the primary and secondary cyclones. From 00 UTC 16th until 06 UTC 17 April, primary cyclone moved eastward-southeastward with an average speed of 11.5 m s^{-1} , which is typical of this type of system over South Atlantic (Reboita, 2008). Afterwards it underwent fast southeastward displacement until 18 UTC 17 April. From its first position on 06 UTC 17 April, the secondary cyclone presents slow movement to the eastward/southeastward (Figure 3) with a total life time of about five days.

3.2 Stratospheric Intrusion

Figure 4a shows that, at 300 hPa, the PV anomaly, characterized by contours lower than -1.5 PVU, also corresponds to areas with relative humidity lower than 10%. Figure 4b displays a vertical cross

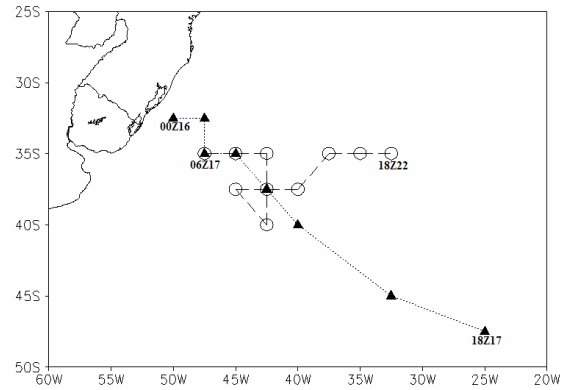


Figure 3. Track of the cyclones with its respective date (hour, hh, and day, dd) from genesis and dissipation for primary (----Δ----) and secondary (----○----) cyclone.

section along 55° W longitude at 00 UTC April 17 (indicated by solid line in Figure 4a). This section crosses the 300 hPa PV anomaly and shows the \mathbf{Q} -vector divergence. A large area of the sinking motion, characterized by \mathbf{Q} -vector divergence from the stratosphere to 700 hPa, is found in the north of the PV anomaly. Below and on the northern sector of PV anomaly, the horizontal gradient of potential temperature is intense, exhibiting a strong baroclinic region at low levels.

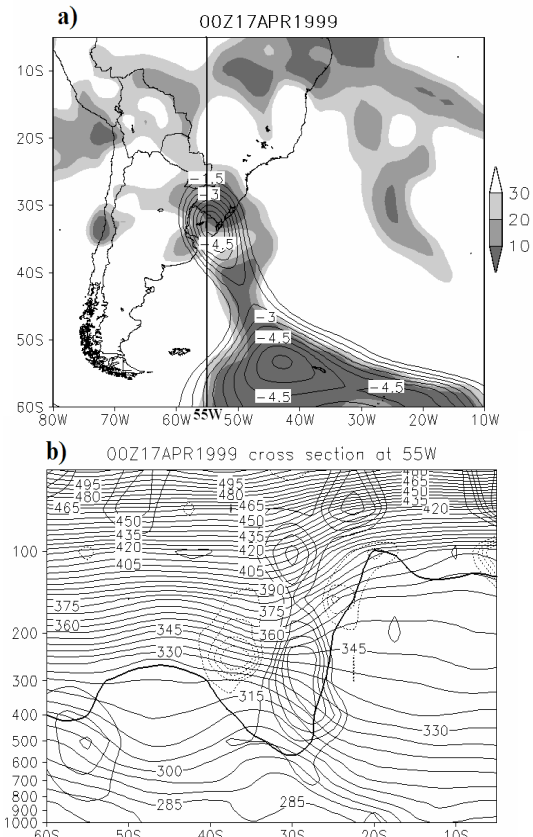


Figure 4. a) Relative humidity (% shaded gray) and potential vorticity (solid line, every 0.5 PVU) at 300 hPa. The straight line along 55° W longitude indicates the location of the vertical cross section in b). b) \mathbf{Q} -vector divergence ($\times 10^{-15} \text{ m s}^{-1} \text{ kg}^{-1}$, solid line is positive and dotted is negative) and potential temperature (thin solid lines, every 5 K) and -1.5 PVU (heavy solid line).

As shown in Figure 5, the TOMS data exhibit greater amounts of ozone in the region of the PV anomaly showed in Figure 4a. This indicates that a stratospheric ozone intrusion associated with sinking motion in the PV anomaly region was occurring (Figure 4a). The agreement between greater values of ozone in a column and PV anomaly are also reported in other works such as Danielsen (1968), Uccellini et al. (1985), Ramamurthy and Xu (1994) and Davies and Schuepbach (1994).

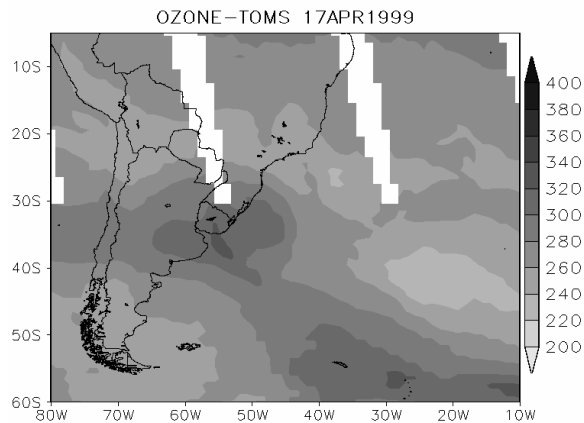


Figure 5. TOMS ozone total (DU) at 1120 UTC 17 April 1999.

3.3 Warming Anomaly at 200 hPa

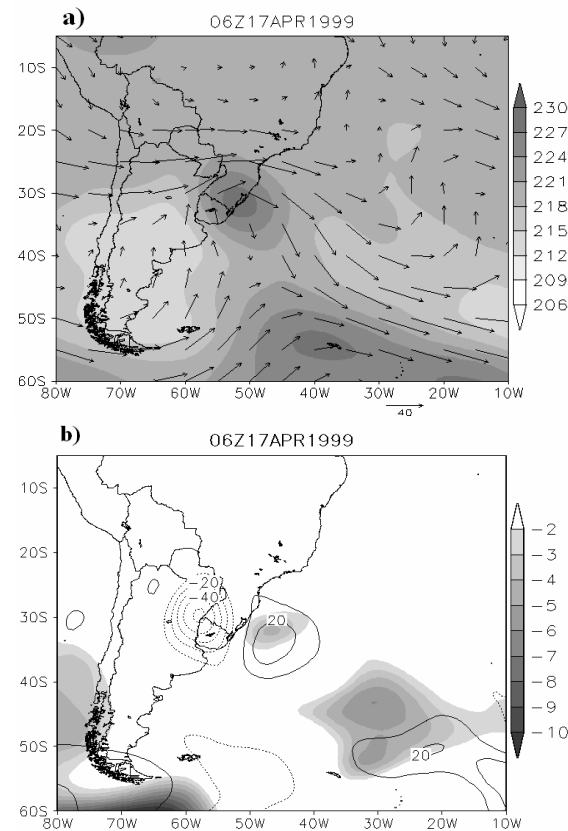


Figure 6. a) Temperature (K, shaded gray), and horizontal wind (m s^{-1} , vector) at 200 hPa at 06 UTC 17 April. b) Geopotential height tendency at 1000 hPa (m h^{-1} , shaded gray showing only negative values), and temperature advection at 200 hPa (K day^{-1} , solid line is positive and dotted line is negative) at 06 UTC 17 April.

Hirschberg and Fritsch (1991) report the tropopause undulation region as being characterized by a warm anomaly at 200 hPa. Figure 6a display the air temperature and horizontal wind at 200 hPa at 06 UTC 17 April. Figure 6a shows that the secondary cyclone developed in the polar side of the maximum wind speed at 200 hPa. Relatively warm air (Figure 6a) coincides with the PV anomaly at 300 hPa (Figure 2) throughout the life cycle of the secondary cyclone. This warm anomaly is accompanied by cold anomalies to the southwest and southeast. In the tropopause and stratosphere, the static stability is normally high, such that a small vertical motion may cause great changes in temperature. At this times, 06 UTC 17 April, the localization of the cold and warm anomalies favored cold and warm advection, respectively, in the western and eastern side 200 hPa warm anomaly (Figure 6b). As discussed by Hirschberg and Fritsch (1991), surface low pressure systems can develop below upper level warm advection and the falls of 1000 hPa geopotential height due to the warming of the atmospheric column (Figure 6b).

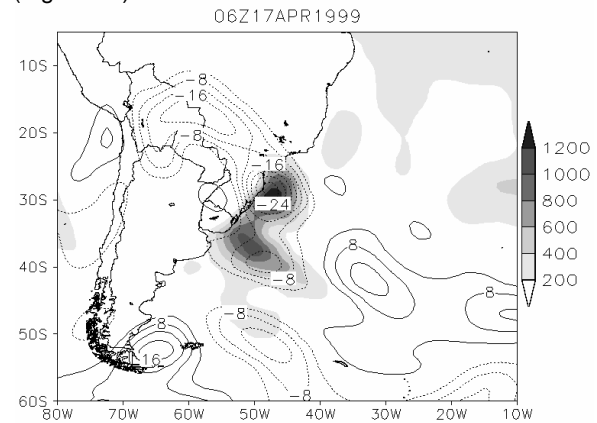


Figure 7. Temperature advection (K s^{-1} , solid line is positive and dotted is negative) at 1000 hPa, and total surface flux (latent plus sensible heat flux) (W m^{-2} , shaded gray showing only positive flux) by 06 UTC 17 April 1999.

Figure 7 displays an intense total heat flux in opposition to strong cold advection in the development region of secondary cyclone. The total flux on surface can be contributed to destabilize the atmosphere near surface.

4. Conclusion

The stratospheric air intrusion to the tropospheric levels was confirmed through the PV anomaly features at 300 hPa, extending vertically until the mid troposphere. Downward vertical motions were diagnosed through the \mathbf{Q} -vector divergence. The PV anomaly was associated with a warm anomaly above 200 hPa. The advection of this warm anomaly to the eastern sector of the 300 hPa PV core contributed to the 1000 hPa geopotential fall. Therefore, the development of secondary cyclone can be due coupling between the cyclonic circulation at upper level and total heat flux near surface.

5. References

- Ancelet, G., J. Pelon, M. Beekmann, A. Papayannis, and G. Megie (1991), Ground-based lidar studies of ozone exchanges between the stratosphere and the troposphere, *J. Geophys. Res.*, *96*, D(12), 22401-22421.
- Bluestein, H. (1993), *Synoptic-Dynamic Meteorology in Midlatitudes: Observations and Theory of Weather Systems*, vol. 2, 594 pp., Oxford University Press. New York.
- Bosart, L. (1999), Observed cyclone life cycles. The life cycles of extratropical cyclones (M. A. Shapiro and D. Gronas, Eds), *Amer. Meteor. Soc.*, 187-213.
- Danielsen, E. F. (1968), Stratospheric-tropospheric exchange based upon radioactivity, ozone and potential vorticity, *J. Atmos. Sci.*, *25*, 502-518.
- Danielsen, E. F., and V. A. Mohnen (1977), Project Dustorm report: Ozone transport, in situ measurements, and meteorological analyses of tropopause folding, *J. Geophys. Res.*, *82*, 5867-5877.
- Davies, H. C., C. Schär, and H. Wernli (1991), The palette of fronts and cyclones within a baroclinic wave development, *J. Atmos. Sci.*, *48*, 1666-1689.
- Davies T. D., and E. Schuepbach (1994), Episodes of high ozone concentrations at the earth's surface resulting from transport down from the upper troposphere/lower stratosphere: A review and case studies, *Atmos. Environ.*, *28*, 53-68.
- Miky-Funatsu, B., M. A. Gan, and E. Caetano (2004), A case study of orographic cyclogenesis over South America, *Atmósfera*, *17-2*, 91-113.
- Hirschberg, P. A., and J. M. Fritsch (1991), Tropopause undulations and the development of extratropical cyclones, Part I: Overview and observations from a cyclone event, *Mon. Wea. Rev.*, *119*, 496-517.
- Hirschberg, P. A., and J. M. Fritsch (1991), Tropopause undulations and the development of extratropical cyclones, Part II: Analysis and conceptual model, *Mon. Wea. Rev.*, *119*, 518-550.
- Holland, G. J., A. H. Lynch, and L. M. Leslie (1987), Australian east-coast cyclones. Part I: Synoptic overview and case study, *Mon. Wea. Rev.*, *115*, 3024-3036.
- Hoskins, B. J., I. Draghici, and H. C. Davies (1978), A new look at the ω -equation, *Q. J. R. Meteorol. Soc.*, *104*, 31-38.
- Hoskins, B. J., M. E. McIntyre, and W. Robertson (1985), On the use and significance of isentropic potential vorticity maps, *Q. J. R. Meteorol. Soc.*, *111* (470) 877-946.
- Kanamitsu, M., W. Ebisuzaki, J. Woollen, S. K. Yang, J. J. Hnilo, M. Fiorino, and G. L. Potter (2002), NCEP-DOE AMIP-II Reanalysis (R-2), *Bull. of the American Met. Soc.*, November, 1631-1643.
- Ramamurthy, M. K., and T. -Y. Xu (1994), Structure and evolution of a tropopause fold during GALE IOP-1: An Eta model study, *Meteorol. Atmos. Phys.*, *53*, 161-183.
- Reboita, M. S. (2008), Ciclones Extratropicais sobre o Atlântico Sul: Simulação Climática e Experimentos de Sensibilidade, Meteorology Ph.D. Dissertation, Institute of Astronomy, Geophysics and Atmospheric Sciences – IAG–USP, 359 pp.
- Reed, R. J. (1955), A study of a characteristic type of upper-level frontogenesis, *J. Meteor.*, *12*, 226-237.
- Reed, R. J., and E. F. Danielsen (1959), Fronts in the vicinity of the tropopause, *Arch. Meteor. Geophys. Bioklim.*, *A11*, 1-17.
- Ronadanelli, R., L. Gallardo, and R. D. Garreaud (2002), Rapid change in ozone mixing ratios at Cerro Tololo (30°10'S, 70°48'W, 2200m) in connection with cutoff lows and deep troughs, *J. Geophys. Res.*, *107*, (D23), 4677.
- Satyamurty, P., J. F. B. Fonseca, M. J. Bottino, M. E. Seluchi, M. C. M. Lourenço, and L. G. G. Gonçalves (2002), An early freeze in southern Brazil in April 1999 and its NWP guidance, *Meteorol. Appl.*, *9*, 113-128.
- Thorncroft, C. D., B. J. Hoskins, and M. E. McIntyre (1993), Two paradigms of baroclinic-wave life-cycle behaviour, *Q. J. R. Meteorol. Soc.*, *119*, 17-55.
- Uccellini, L. W., D. Keyser, K. F. Brill, and C. H. Wash (1985), The President's Day cyclone of 18-19 February 1979: Influence of upstream trough amplification and associated tropopause folding on rapid cyclogenesis. *Mon. Wea. Rev.*, *113*, 962-988.